ORIGINAL ARTICLE

WILEY

Comparison of magnetic resonance imaging and computed tomography to measure preoperative parameters of children with pectus excavatum

Jihang Sun[1*] | Chenghao Chen[2*] | Yun Peng[1] | Yue Zhang[1] | Hongwei Tian[1] | Jie Yu[2] | Jun Cao[3] | Qi Zeng[2]

[1]Imaging Center, Beijing Children's Hospital, Capital Medical University, National Center for Children's Health, Beijing, China
[2]Department of Thoracic Surgery, Beijing Children's Hospital, Capital Medical University, National Center for Children's Health, Beijing, China
[3]Department of Orthopedics, Beijing Children's Hospital, Capital Medical University, National Center for Children's Health, Beijing, China

Correspondence
Yun Peng, Imaging Center, Beijing Children's Hospital, Capital Medical University, National Center for Children's Health, Beijing, China.
E-mail: ppengyun@yahoo.com
Qi Zeng, Department of Thoracic Surgery, Beijing Children's Hospital, Capital Medical University, National Center for Children's Health, Beijing, China.
Email: zengqi-1@163.com

[*]These authors contributed equally to this work.

Received: 7 January, 2018
Accepted: 5 March, 2019

ABSTRACT

Importance: Pectus excavatum (PE) is the most common thoracic wall deformity in children, we need a method which could be used to evaluate pulmonary functions and effects on development.

Objective: To evaluate the use of 3D T1-weighted (3DT1) and mDIXON magnetic resonance imaging (MRI) sequences for measuring the thoracic parameters and morphology of children with PE, comparing the measurements with those made on computed tomography (CT).

Methods: This is a retrospective study of children with thoracic deformities who were hospitalized at the Department of Thoracic Surgery of the Heart Center, Beijing Children's Hospital, between June 2014 and June 2015. Chest CT was performed first, with the MRI scanning then being performed 0–3 days later. The mDIXON sequences were obtained in inspiratory and expiratory phases and the 3DT1 sequences were obtained during free breathing. Thoracic volume was measured using the acquired images.

Results: The lung volumes measured on mDIXON MRI and CT were highly correlated, with the Haller index not being significantly different between the two methods. Bland-Altman analyses showed that lung, cardiac, and retrosternal parameters were similar between the two methods. Pulmonary parameters were higher with the end-inspiratory phase mDIXON images than with the end-expiratory phase images, as expected, while cardiac parameters were unaffected by the respiratory phase.

Interpretation: Thoracic volumes measured on mDIXON MRI in combination with held respiration could reflect lung volume functions and help in observing the movement functions of the lungs and heart. The method could be used instead of CT, avoiding subjecting the patient to potentially harmful radiation.

KEYWORDS

Lung volume measurements, Magnetic resonance imaging, Thoracic wall, X-ray computed tomography

DOI: 10.1002/ped4.12132

INTRODUCTION

Pectus excavatum (PE) is the most common thoracic wall deformity in children, accounting for about 90% of all juvenile thoracic wall deformities.[1,2] PE not only affects the appearance of the thoracic wall due to koilosternia, but can also affect the mental health of affected children.[1,3,4] In recent years, thoracic insufficiency syndrome (TIS) has attracted increasing attention, mainly because of the compression of lungs, heart, and large mediastinal vessels from deformities of the sternum and costal cartilages, which reduce thoracic volume and in turn limit lung inflation, affect alveoli development and formation, and influence respiratory functions and heart and lung development; thus resulting in persistent effects on the growth of children.[5]

Therefore, the indications for operations to correct thoracic deformities and the associated evaluation criteria have gradually changed from improving the cosmetic appearance and Haller index (HI), to improving pulmonary functions and effects on development.[6] Conventional pulmonary function tests (PFT)[7] do not meet the requirements for appropriate management of PE; therefore, clinicians now use computed tomography (CT) volume reconstruction as the gold standard for obtaining more detailed data on pulmonary functions.[8,9] It has been demonstrated that both inspiratory and expiratory CT have great impacts on the evaluation of thoracic movement.[10,11] Albertal et al[12] showed that assessment of PE at end-expiration led to an additional number of surgical candidates compared with end-inspiration assessment only.

Nevertheless, the effects of the ionizing radiation on the health of children are non-negligible, and magnetic resonance imaging (MRI) is a safer technique for obtaining imaging data for the management of PE.[13-17] However, the acquisition time and motion artifacts are major disadvantages to MRI. The multi-echo 2-point DIXON (mDIXON) scanning sequence is a novel technique that allows for fast scanning that can be completed during breath-holding.[18,19] Furthermore, we noticed that three-dimensional T1-weighted (3DT1) MRI allows chest scanning with free breathing.[20]

Therefore, we sought to use non-invasive MRI examinations to obtain inspiratory and expiratory phase lung volume measurements in children with PE, and compared the results with volume reconstructions of thoracic CT scanning. We hypothesized that if the non-invasive MRI examination could be used to evaluate lung volume, we could obtain more comprehensive results while avoiding the potential radiation damage caused by CT scanning.

METHODS

Study design and patients

This is a retrospective study of children with thoracic deformities who were hospitalized at the Department of Thoracic Surgery of the Heart Center Beijing Children's Hospital between June 2014 and June 2015. The inclusion criteria were: 1) thoracic deformities and a need for surgical correction (CT examination showed a HI > 3.0, and/or the child and parents strongly required surgical correction); 2) an age of 6 years or above to ensure active cooperation in the pulmonary function test, CT scanning, and magnetic resonance (MR) examination; and 3) without a history of respiratory infection in the last 2 months. The exclusion criteria were: 1) a history of respiratory infection within the past 2 months or with chronic respiratory diseases; 2) other deformities that could change the pulmonary volume (e.g., congenital bronchopulmonary cystic abnormalities); or 3) used drugs before and/or after hospitalization, or received treatments that could change pulmonary ventilation.

The present study was approved by the Ethics Committee of Beijing Children's Hospital. The legal guardians of all children signed written informed consent.

Chest CT scanning

Chest CT was performed first, followed by the MRI scanning 0–3 days later. A 64-row CT system (LightSpeed VCT64, GE Healthcare, Waukesha, WI, USA) was used for the chest CT scanning. The parameters included: slice thickness of 0.625 mm, slice gap of 0.625 mm, matrix of 512 × 512, voltage of 120 kV, and automatic current adjustment. The CT scanning started at the thoracic entrance and covered the whole of the costal cartilages.

Chest MRI

All MRI scans were performed on a Philips Ingenia 1.5-T magnetic resonance scanner (Philips, Best, The Netherland) with a 32-channel digital body coil. During scanning, the children were placed in the supine position, with their hands upheld to avoid artifacts. Upholders were placed on both sides of the thorax to prevent the coil from directly oppressing the child's chest. The scanning volume covered the area from the thoracic entrance to the lower margin of the costal arch, that is, the whole thorax. For the mDIXON sequence, the parameters included a matrix of 180 × 180, voxel acquisition of 2mm × 2mm × 2 mm, flip angle of 15°, and NeX (number of excitations) of one. The children were asked to hold their breath after inspiration for the 12 s acquisition of the inspiratory phase mDIXON image (MRin), then, after a short break, the scanning was repeated after expiration to obtain the expiratory phase mDIXON image (MRex). For the 3DT1 sequence, the matrix was 152 × 127, the flip angle 25°, and images were collected with four NeX. The patients were not required to hold their breath during the 3DT1 scanning, with the sequence acquisition times being 120–180 s, according to the child's body size.

Image processing

As the CT and MRI images were distinct, blinding could not be applied in respect to the imaging modality. To partially overcome this problem, the image analysis was performed 2 months after scanning. In addition, personal information on the screen was covered, and the images were shuffled by a technician.

MR image processing

After completing the scanning, the MRI and CT data were uploaded into AW4.5 workstation software (GE Healthcare, Waukesha, WI, USA). The "hand sketching method" described by Schlesinger and Hernandez[21] was used for analysis of the MRI data (Figure 1). Briefly, a mouse was used to manually outline the margins of the lungs of the left and right thorax on axial images, so as to include all the closed lung regions. This process was performed by two clinicians; one was a radiologist with 9 years of experience and the other was a thoracic surgeon with 9 years of experience in thoracic deformities in children. Any disagreement between the two physicians was solved by discussion, resulting in a single drawing and not the average of two drawings. Then, enhancing tools provided by the workstation were applied to automatically recognize the lung margins and calculate the volume. The workstation could also automatically overlay the data from the hand-sketching levels to obtain the left lung volume (Lvol), right lung volume (Rvol), and total lung volume (Tvol). MR functional volumes (FV) of the left, right, and total lung (L, R, and T) were calculated from the volumes in the inspiratory phase minus the volumes in the expiratory phase. The lung movement function (LMF) of the left, right, and total lung (L, R, and T) was calculated according to the following equation: LMF = FV/Vol.

CT image processing

CT scanning data were processed using the workstation, including threshold restriction and volume rendering (VR) for three-dimensional lung modeling (3D-lung). The thoracic volumes of the children were automatically calculated by the software using Hounsfield unit thresholds of −1024 to −200. The HI values of the CT images were also evaluated, with the distance from the lowest point of the sternum to the anterior vertebral edge (anteroposterior diameter, APD) and the transverse diameter (TD) being measured, and the HI being calculated as TD/APD. The distances from the lung apex to the points on different planes at the level of the tracheal carina were measured on coronal images to obtain left lung height (LLH), right lung height (RLH), and mean lung height (MLH, the mean value of LLH and RLH).

The morphological data of the heart at the most oppressed level were measured, including the minimum vertical cardiac diameter, minimum anteroposterior diameter (MinAP), maximum anteroposterior diameter (MaxAP, at the scanning level), left heart diameter (LHD, the distance from the left margin of the heart to the midline of the chest), right heart diameter (RHD, the distance from the right margin of the heart to the midline of the chest), heart transverse diameter (HTD, = LHD + RHD), cardiac compression index (CCI, = HTD/MinAP), heart rotation angle (HRA, the angle between MinAp and a line from the left cardiac margin to the anterior spinal margin), and chest anteroposterior diameter (CAPD, the distance from the posterior margin of the sternum to the anterior spinal margin). Data were measured on the 3DT1, MRin, MRex, and CT images (Figure 1).

Statistical analysis

Normally distributed data are presented as means ± standard deviation and were analyzed using Student's *t*-test. Non-normally distributed data are presented as median (range) and were analyzed using the Kruskal-Wallis test. Categorical data are presented as frequencies and were analyzed using the chi-square test. The Bland-Altman method was used to examine the consistencies between MRI and CT. All analyses were carried out using SPSS 16 for Windows (IBM, Armonk, NY, USA). Two-sided *P*-values < 0.05 were considered statistically significant.

RESULTS

Characteristics of the patients

A total of 41 children (33 males and 8 females, with a mean age of 12.4 ± 2.6 years, ranging from 6 to16 years) were enrolled. The characteristics of the patients are present in Table 1. The average CT radiation dose was 4.37 ± 1.53 mGy.

TABLE 1 Patients' characteristics (*n* = 41)

Parameters	Characteristics
Age (years)	12.4 ± 2.6
Gender	
Male	33 (80.5)
Female	8 (19.5)
Height (cm)	156.1 ± 15.2
Weight (kg)	42.4 ± 10.6
Body mass index	17.1 ± 2.1
Type of disease	
Central	30 (73.2)
Bilateral	5 (12.2)
Flat chest	6 (14.6)
Direction of sternum dislocation	
No dislocation, sternum depressed downward	36 (87.8)
Sternum depressed toward lower left	2 (4.9)
Sternum depressed toward lower right	3 (7.3)

Data are presented as mean ± SD or *n* (%).

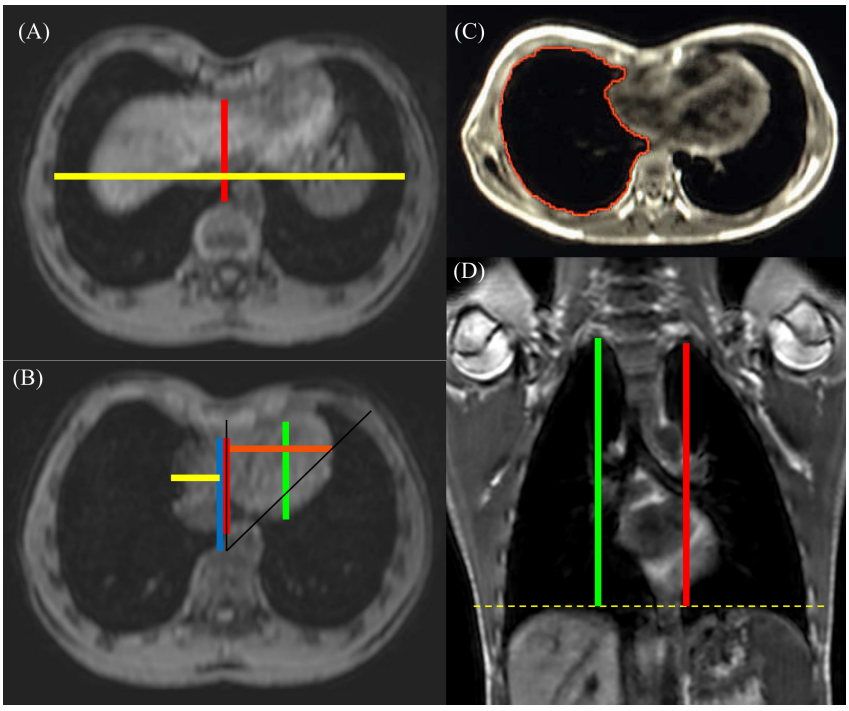

FIGURE 1 "Hand sketching method" used for the analysis of MRI data. (A) An inspiratory phase mDIXON image (MRin) at the most depressed level of the sternum. The red line from the lowest point of the most depressed level of the sternum indicates the distance from the sternum to the anteroposterior margin of the spine (anteroposterior diameter, APD). The yellow line is the transverse diameter (TD). The HI was calculated as TD/APD. (B) MRin image from the most oppressed level of the heart. The red line shows the minimum vertical cardiac diameter and anteroposterior (MinAP), the green line the maximum anteroposterior (MaxAP), the orange line the left heart diameter (LHD), and the yellow line the right heart diameter (RHD). The heart transverse diameter (HTD) was calculated as LHD + RHD. The cardiac compression index (CCI) was calculated as HTD/MinAP. The black line shows the heart rotation angle (HRA), and the blue line the chest anteroposterior diameter (CAPD). (C) MR3DT1 image showing the left lung volume measured using the hand-sketching of this layer. (D) MR3D coronal image at the level of the tracheal carina. The yellow dashed line represents a horizontal at the top of diaphragm. The right diaphragmatic surface level is basically in accordance with the left level. The red vertical line shows the left lung height (LLH) and the green line shows the right lung height (RLH). The mean lung height was calculated as the mean value of LLH and RLH.

Comparisons between CT and MRI

The CT and MR acquisitions were compared by creating Bland-Altman charts of lung volume, lung height, HI, and cardiac diameters (Table 2). The Bland-Altman charts showed that the CT and MRI measurements of Tvol (Figure 2A), Rvol (Figure 2B), Lvol (Figure 2C), LLH (Figure 2D), RLH (Figure 2E), MLH (Figure 2F), APD (Figure 2G), TD (Figure 2H), HI (Figure 2I), MinAP (Figure 3A), MaxAP (Figure 3B), RHD (Figure 3C), LHD (Figure 3D), HTD (Figure 3E), HRA (Figure 3F), CCI (Figure 3G), and CAPD (Figure 3H) had good consistency.

Comparison of mDIXON MRI according to respiratory phases

Table 3 shows that the pulmonary parameters were higher in the end-inspiratory phase than in the end-expiratory phase, as expected, while the cardiac parameters were unaffected by the respiratory phase.

DISCUSSION

CT is the gold standard for evaluation of the chest in children with PE, including measurement of the volume of lung parenchyma, but the exposure to ionizing radiation remains an issue.[8,9] Although we used low radiation CT techniques and minimized the CT radiation dose, CT is still harmful to children, because they are more sensitive to the ionizing radiation; therefore we wish to replace the routine use of CT in PE. With the better understanding of PE achieved in recent years, the focus of surgical evaluations for thoracic deformities has changed from simply improving the cosmetic appearance to improving lung function.[6,7] Historically, PE was evaluated with the PFT, but the results could not reflect the volume of the individual sides of the lung, which limited its utility.[6,7] In recent years, authors have developed CT-based volume reconstruction techniques to evaluate pulmonary functions,[6,7] including dynamic volume CT.[12] However, although dynamic volume CT can evaluate pulmonary function, it results in a high CT radiation dose, so we have not adopted this method for use in children. Therefore, we considered that MRI could be an appropriate alternative to CT in children with PE, and this study aimed to use 3DT1 and mDIXON MR images instead of CT, avoiding the

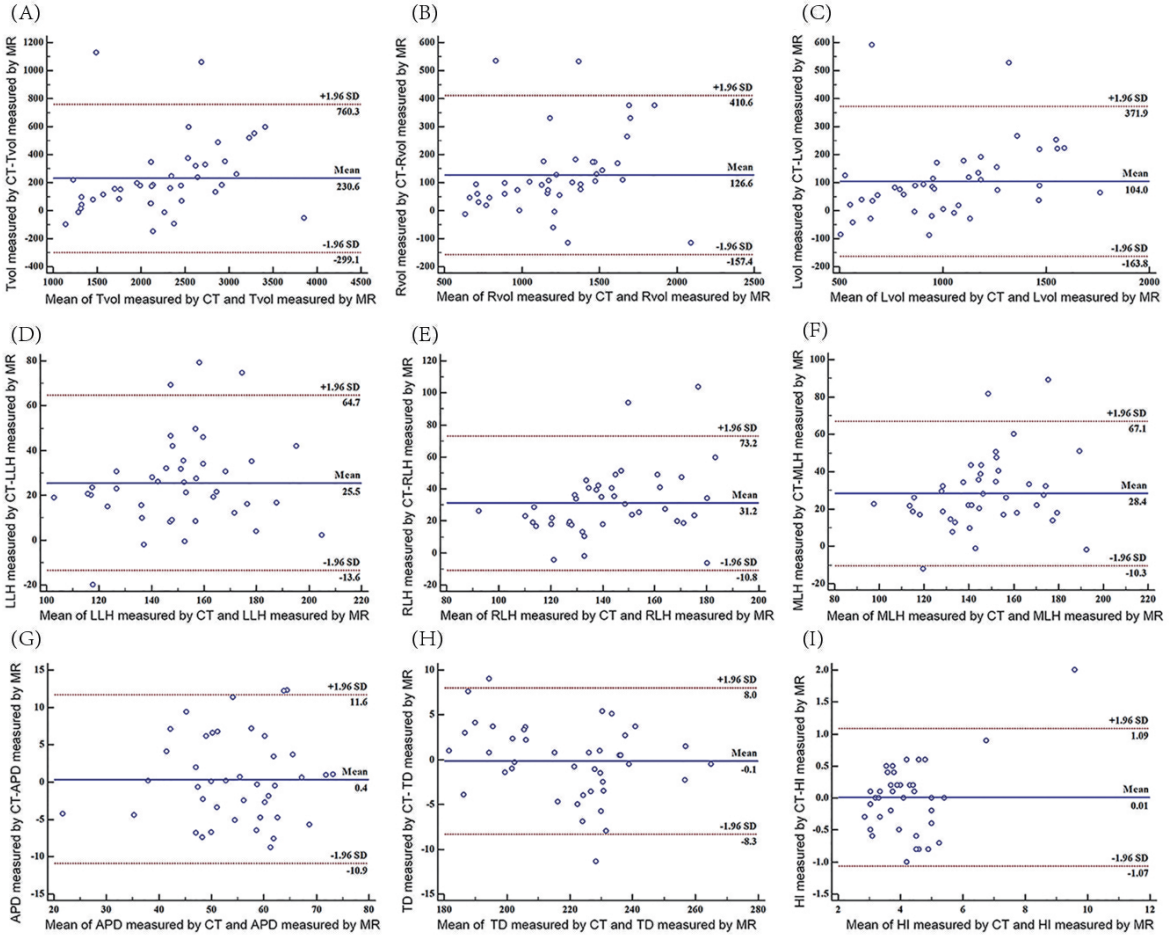

FIGURE 2 Bland-Altman charts of lung volume, lung height, and Haller index measured by CT and MRI. (A) Total lung volume (Tvol). (B) Right lung volume (Rvol). (C) Mean value of the left lung volume (Lvol). (D) Left lung height (LLH). (E) Right lung height (RLH). (F) Mean lung height (MLH). (G) Anteroposterior diameter (APD). (H) Transverse diameter (TD). (I) Haller index (HI).

potential damage from radiation. As the 3DT1 sequence is a conventional technique, it can be used on scanners from different vendor's, and the sequence does not need the subject to perform breath-holding. The mDIXON MRI can be acquired in the inspiratory and expiratory phases to allow measurement of thoracic parameters and morphology, permitting accurate evaluation of pulmonary function in children with PE within a short time.

This study showed that the HI values were not significantly different between 3DT1 and CT images, and that the lung volume results had good consistency, suggesting that the 3DT1 sequence could be used to replace CT scanning for assessment of lung volume, although MRI cannot be used to assess the skeletal system. In addition, mDIXON sequences acquired at different respiratory phases could help understand the pulmonary functions of children with PE. Our results showed that thoracic volumes measured using mDIXON MRI in combination with held respiration can reflect lung volume functions and help in observing the movement functions of the lungs and heart. In addition, for the mDIXON sequence measurements, cardiac parameters were unaffected by the respiratory phase, although the pulmonary parameters were of course higher in the end-inspiratory phase than in the end-expiratory phase. These results are supported by previous studies; indeed, it has been demonstrated that both inspiratory and expiratory CT have great impacts on the evaluation of thoracic movements.[10,11] Albertal et al[12] showed that assessment of PE at end-expiration led to an additional number of surgical candidates compared with end-inspiration assessment. This will have to be validated for the MRI results.

Previous studies have used a variety of MRI sequences for examination of children with PE. Indeed, Piccolo et al[13] showed that fast MRI sequences could be used for the evaluation of children with PE. Similar results were obtained by Lollert et al[14] using T2-HASTE/inspiration and expiration, T2-TRUFI free-breathing, and T2-BLADE sequences; by Burkemeier et al[15] using a fast MRI protocol; by Marcovici et al[16] using a single-axial 2D

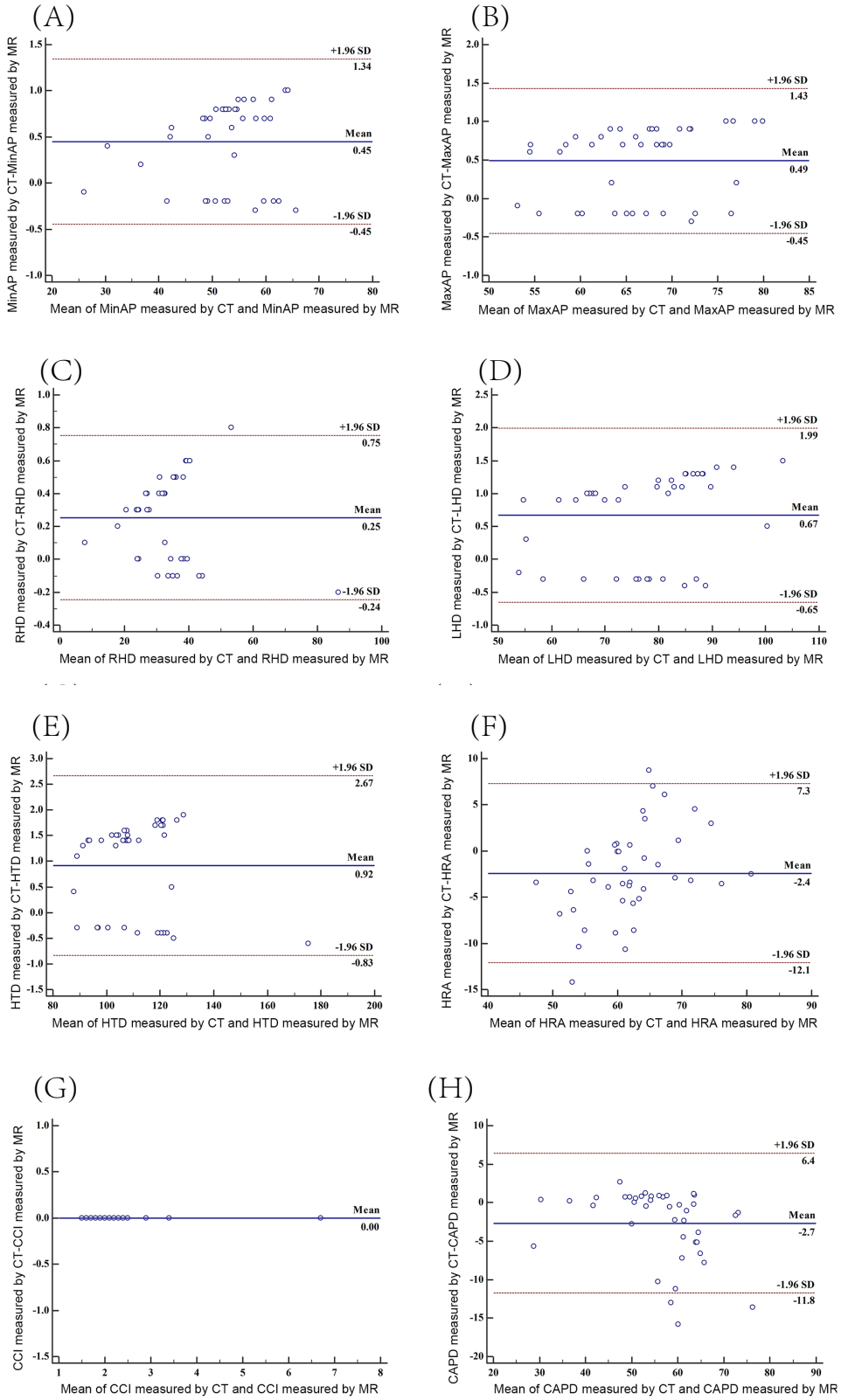

FIGURE 3 Bland-Altman charts of cardiac diameters measured by CT and MRI. (A) Minimum anteroposterior diameter (MinAP). (B) Maximum anteroposterior diameter (MaxAP). (C) Right heart diameter (RHD). (D) Left heart diameter (LHD). (E) Heart transverse diameter (HTD). (F) Heart rotation angle (HRA). (G) Cardiac compression index (CCI). (H) Chest anteroposterior diameter (CAPD) at heart level.

TABLE 2 CT and 3DT1 MRI values of each parameter

Parameter	CT	MRI	Difference	95% *CI*
Total lung volume (Tvol, mm^3)	2372.77 ± 720.23	2142.17 ± 640.90	230.60 ± 270.27	(−299.13, 760.33)
Right lung volume (Rvol, mm^3)	1289.93 ± 377.54	1163.35 ± 341.26	126.58 ± 144.89	(−157.40, 410.56)
Left lung volume (Lvol, mm^3)	1082.84 ± 357.60	978.82 ± 313.90	104.02 ± 136.65	(−163.81, 371.85)
Right lung height (RLH, mm)	158.29 ± 27.58	127.06 ± 21.08	31.23 ± 21.44	(−10.79, 73.25)
Left lung height (LLH, mm)	163.98 ± 26.10	138.43 ± 22.95	25.54 ± 19.96	(−13.58, 64.66)
Mean lung height (MLH, mm)	161.16 ± 26.04	132.77 ± 21.41	28.38 ± 19.74	(−10.31, 67.07)
Anterioposterior diameter (APD, mm)	54.76 ± 10.86	54.40 ± 10.56	0.36 ± 5.76	(−10.93, 11.65)
Transverse diameter (TD, mm)	219.11 ± 20.17	219.26 ± 21.40	−0.15 ± 4.16	(−8.30, 8.00)
Haller index (HI)	4.22 ± 1.32	4.21 ± 1.07	0.01 ± 0.55	(−1.07, 1.09)
Minimum anteriopesterior diameter (MinAP, mm)	52.71 ± 8.48	52.26 ± 8.41	0.45 ± 0.46	(−0.45, 1.35)
Maximum anterioposterior diameter (MaxAP, mm)	67.10 ± 7.23	66.60 ± 7.11	0.49 ± 0.48	(−0.45, 1.43)
Right heart diameter (RHD, mm)	33.43 ± 11.68	33.17 ± 11.71	0.25 ± 0.25	(−0.24, 0.74)
Left heart diameter (LHD, mm)	77.83 ± 12.28	77.16 ± 12.09	0.67 ± 0.67	(−0.64, 1.98)
Heart transverse diameter (HTD, mm)	111.26 ± 15.49	110.34 ± 15.60	0.92 ± 0.89	(−0.82, 2.66)
Heart rotation angle (HRA, °)	60.86 ± 8.27	63.26 ± 6.28	−2.40 ± 4.93	(−12.06, 7.26)
Cardiac compression index (CCI)	2.21 ± 0.83	2.21 ± 0.83	0.00 ± 0.00	N/A
Chest anteroposterior diameter at heart level (CAPD, mm)	54.95 ± 9.67	57.63 ± 11.20	−2.69 ± 4.64	(−11.78, 6.40)

N/A, not applicable; *CI*, confidence interval.

TABLE 3 Comparisons of mDIXON MRI measurements of pulmonary and cardiac diameters between inspiratory and expiratory phases

MRI parameters	Expiratory phase	Inspiratory phase	Difference	95% *CI*
Total lung volume (Tvol, mm^3)	1833.31 ± 576.06	3552.07 ± 1114.91	1718.76 ± 753.63	(241.64, 3195.87)
Right lung volume (Rvol, mm^3)	1013.53 ± 305.51	1906.36 ± 592.45	892.84 ± 395.04	(118.55, 1667.12)
Left lung volume (Lvol, mm^3)	819.79 ± 285.32	1645.70 ± 536.17	825.92 ± 362.32	(115.78, 1536.06)
Anterioposterior diameter (APD, mm)	49.89 ± 10.97	65.51 ± 14.25	15.62 ± 8.69	(−1.41, 32.66)
Transverse diameter (TD, mm)	216.22 ± 19.84	226.79 ± 21.96	10.57 ± 5.61	(−0.44, 21.57)
Haller index	4.60 ± 1.35	3.63 ± 0.87	−0.98 ± 0.72	(−2.39, 0.44)
Right lung height (RLH, mm)	118.19 ± 21.91	169.78 ± 25.21	51.60 ± 18.06	(16.19, 87.00)
Left lung height (LLH, mm)	132.14 ± 24.31	177.35 ± 26.07	45.20 ± 16.35	(13.16, 77.25)
Mean lung height (MLH, mm)	125.19 ± 22.77	173.59 ± 25.36	48.40 ± 16.84	(15.38, 81.41)
Maximum anterioposterior diameter (MaxAP, mm)	50.77 ± 9.91	54.07 ± 8.25	3.30 ± 6.91	(−10.24, 16.84)
Minimum anterioposterior diameter (MinAP, mm)	66.63 ± 8.30	66.99 ± 6.85	0.36 ± 5.33	(−10.09, 10.81)
Right heart diameter (RHD, mm)	32.51 ± 11.75	34.06 ± 12.55	1.54 ± 6.29	(−10.78, 13.87)
Left heart diameter (LHD, mm)	83.39 ± 13.51	71.27 ± 12.08	−12.12 ± 8.31	(−28.41, 4.18)
Heart transverse diameter (HTD, mm)	115.90 ± 16.30	105.33 ± 16.28	−10.57 ± 9.18	(−28.57, 7.43)
Heart rotation angle (HRA, °)	66.26 ± 6.47	60.53 ± 6.75	−5.73 ± 4.06	(−13.69, 2.22)
Cardiac compression index (CCI)	2.43 ± 0.96	2.04 ± 0.78	−0.39 ± 0.43	(−1.23, 0.44)
Chest anteroposterior diameter at heart level (CAPD, mm)	52.33 ± 11.01	66.87 ± 14.28	14.54 ± 9.99	(−5.05, 34.13)

CI, confidence interval.

FIESTA protocol; and by Humphries et al[17] using cardiac MRI sequences. All these sequences are fast imaging sequences and allow images to be acquired in a short time with the avoidance of motion artifacts. Despite the variety of different sequences being used, all of these studies, as well as the present one (which used 3DT1 and mDIXON sequences), showed that MRI was appropriate for the evaluation of PE in children. However, additional studies

are necessary to compare the different sequences.

Although the findings of the present study are encouraging, there are still several limitations to this study. First, the sample size was relatively small, and the children were all of school age (> 6 years old). Second, the children were asked to uphold their upper arms during MR and CT scanning, because of limitations with the examination methods. This position was slightly different to the supine position, and could have affected the shape and movement pattern of the thorax. Third, the MRI results showed that the movement range and thoracic volume of the bilateral lungs were uneven, although the exact reasons for this were not identified.

In conclusion, the thoracic volumes measured by mDIXON MRI in combination with held respiration can reflect lung volume functions, and help in observing the movement functions of the lungs and heart. The method could be used instead of CT, avoiding the potential damage from ionizing radiation.

CONFLICT OF INTEREST

There are no conflicts of interest.

REFERENCES

1. Kelly RE Jr, Lawson ML, Paidas CN, Hruban RH. Pectus excavatum in a 112-year autopsy series: anatomic findings and the effect on survival. J Pediatr Surg. 2005;40:1275-1278.
2. Willital GH, Saxena AK, Schutze U, Richter W. Chest-deformities: a proposal for a classification. World J Pediatr. 2011;7:118-123.
3. Lam MW, Klassen AF, Montgomery CJ, LeBlanc JG, Skarsgard ED. Quality-of-life outcomes after surgical correction of pectus excavatum: a comparison of the Ravitch and Nuss procedures. J Pediatr Surg. 2008;43:819-825.
4. Jacobsen EB, Thastum M, Jeppesen JH, Pilegaard HK. Health-related quality of life in children and adolescents undergoing surgery for pectus excavatum. Eur J Pediatr Surg. 2010;20:85-91.
5. Mayer O, Campbell R, Cahill P, Redding G. Thoracic insufficiency syndrome. Curr Probl Pediatr Adolesc Health Care. 2016;46:72-97.
6. Kelly RE Jr. Pectus excavatum: historical background, clinical picture, preoperative evaluation and criteria for operation. Semin Pediatr Surg. 2008;17:181-193.
7. Kelly RE Jr, Mellins RB, Shamberger RC, Mitchell KK, Lawson ML, Oldham KT, et al. Multicenter study of pectus excavatum, final report: complications, static/exercise pulmonary function, and anatomic outcomes. J Am Coll Surg. 2013;217:1080-1089.
8. Gollogly S, Smith JT, White SK, Firth S, White K. The volume of lung parenchyma as a function of age: a review of 1050 normal CT scans of the chest with three-dimensional volumetric reconstruction of the pulmonary system. Spine. 2004;29:2061-2066.
9. Fayad LM, Johnson P, Fishman EK. Multidetector CT of musculoskeletal disease in the pediatric patient: principles, techniques, and clinical applications. Radiographics. 2005;25:603-618.
10. Gaeta M, Minutoli F, Girbino G, Murabito A, Benedetto C, Contiguglia R, et al. Expiratory CT scan in patients with normal inspiratory CT scan: a finding of obliterative bronchiolitis and other causes of bronchiolar obstruction. Multidiscip Respir Med. 2013;8:44.
11. Hersh CP, Washko GR, Estepar RS, Lutz S, Friedman PJ, Han MK, et al. Paired inspiratory-expiratory chest CT scans to assess for small airways disease in COPD. Respir Res. 2013;14:42.
12. Albertal M, Vallejos J, Bellia G, Millan C, Rabinovich F, Buela E, et al. Changes in chest compression indexes with breathing underestimate surgical candidacy in patients with pectus excavatum: a computed tomography pilot study. J Pediatr Surg. 2013;48:2011-2016.
13. Lo Piccolo R, Bongini U, Basile M, Savelli S, Morelli C, Cerra C, et al. Chest fast MRI: an imaging alternative on pre-operative evaluation of Pectus Excavatum. J Pediatr Surg. 2012;47:485-489.
14. Lollert A, Funk J, Tietze N, Turial S, Laudemann K, Düber C, et al. Morphologic assessment of thoracic deformities for the preoperative evaluation of pectus excavatum by magnetic resonance imaging. Eur Radiol. 2015;25:785-791.
15. Birkemeier KL, Podberesky DJ, Salisbury S, Serai S. Limited, fast magnetic resonance imaging as an alternative for preoperative evaluation of pectus excavatum: a feasibility study. J Thorac Imaging. 2012;27:393-397.
16. Marcovici PA, LoSasso BE, Kruk P, Dwek JR. MRI for the evaluation of pectus excavatum. Pediatr Radiol. 2011;41:757-758.
17. Humphries CM, Anderson JL, Flores JH, Doty JR. Cardiac magnetic resonance imaging for perioperative evaluation of sternal eversion for pectus excavatum. Eur J Cardiothorac Surg. 2013;43:1110-1113.
18. Hussain S, Perkins T. Preliminary clinical experience with a multiecho 2-Point DIXON (mDIXON) sequence at 3T as an efficient alternative for both the SAR-intensive acquired in- and out-of-phase chemical shift imaging as well as for 3D fat-suppressed T1-weighted sequences used for dynamic gadolinium-enhanced imaging. Proc Int Soc Mag Reson Med. 2010;18:556.
19. Eggers H, Brendel B, Herigault G. Comparison of dixon methods for fat suppression in single breath-hold 3D gradient-echo abdominal MRI. Proc Int Soc Mag Reson Med. 2009;17:2705.
20. Hochhegger B, de Souza VV, Marchiori E, Irion KL, Souza AS Jr, Elias Junior, et al. Chest magnetic resonance imaging: a protocol suggestion. Radiol Bras. 2015;48:373-380.
21. Schlesinger AE, Hernandez RJ. Congenital heart disease: applications of computed tomography and magnetic resonance imaging. Semin Ultrasound CT MR. 1991;12:11-27.

How to cite this article: Sun J, Chen C, Peng Y, Zhang Y, Tian H, Yu J, et al. Comparison of magnetic resonance imaging and computed tomography to measure preoperative parameters of children with pectus excavatum. Pediatr Invest. 2019;3:102-109. https://doi.org/10.1002/ped4.12132